

Rotational Libration of a Double-Decker Porphyrin Visualized

Joe Otsuki,^{*,†} Yuji Komatsu,[†] Daiya Kobayashi,[†] Masumi Asakawa,[‡] and Koji Miyake[‡]

College of Science and Technology, Nihon University, 1-8-14 Kanda Surugadai, Chiyoda, Tokyo 101-8308, Japan,
and National Institute of Advanced Industrial Science and Technology, 1-2-1 Namiki, Tsukuba,
Ibaraki 305-856, Japan

Received August 21, 2009; E-mail: otsuki@chem.cst.nihon-u.ac.jp

Molecular rotors are attracting much attention in the pursuit of ever-smaller machines.¹ Studies of double-decker porphyrins in solution have revealed that the two rings undergo rotational libration with respect to each other.^{2,3} The double-decker complexes may be considered among the most promising rotatable components for molecular rotors in view of their amenability to additional functionalization. Thus, visualization of the rotational libration of double-decker complexes on an individual molecule basis is an important means of understanding the rotational dynamics—and finding ways of controlling it. We and others have previously used scanning tunneling microscopy (STM) to observe arrays of double-decker complexes at solid–liquid interfaces on the surfaces of highly oriented pyrolytic graphite (HOPG).^{4,5} Although the rotational libration has been inferred on the basis of the shapes of the observed molecules,⁴ no solid evidence has been presented to date. In this present study, we visualized the rotational libration of a macrocyclic ring within a double-decker porphyrin on an individual-molecule basis.⁶

We prepared a new double-decker porphyrin [Ce(C₂₂OPP)(TPP-Fc)] [TPP-Fc = 5-(4-(4-ferrocenylphenylethynyl)phenyl)-10,15,20-triphenylporphyrin; C₂₂OPP = 5,10,15,20-tetrakis(4-docosyloxyphenyl)porphyrin] featuring a ferrocene unit tethered through a rigid spacer to one of the rings. The STM image in Figure 1, recorded at the HOPG/1-phenyloctane interface, reveals a lamellar pattern composed of larger spots accompanied by smaller dots. We assign the pairs of larger (double-decker core) and smaller (ferrocene moiety) dots to individual double-decker molecules. The intermolecular distances along and across the row of molecules (the larger spots) are 2.1 and 4.6 nm, respectively. Because this two-dimensional lattice is close to that observed for the array of H₂(C₂₂OPP) [5,10,15,20-tetrakis(4-docosyloxyphenyl)porphyrin],^{4a} we assume that the molecules are immobilized on the surface through adsorption of the C₂₂OPP ring, presenting the TPP-Fc ring to the solution. The ferrocene moiety serves as a molecular beacon; it is always located on one side of the row (perpendicular orientation, ⊥), except for positions adjacent to defects.⁷ Consecutive scans of the same area revealed that reorientation of the upper ring, or exchange of molecules on the surface with those in the overlying solution, rarely occurred in the densely packed array.

STM images of a mixture of [Ce(C₂₂OPP)(TPP-Fc)] and H₂(C₂₂OPP) reveal (Figure 2) molecules aligned in the same manner as those in the cases of [Ce(C₂₂OPP)(TPP-Fc)] and H₂(C₂₂OPP) alone. We ascribe the dimmer spots on the rows to the free-base porphyrin. Brighter spots on the rows accompanied by smaller features located on either the left or right side correspond to double-decker porphyrins with a perpendicular ferrocene moiety (⊥); pairs of bright spots on the rows without any feature on their sides are

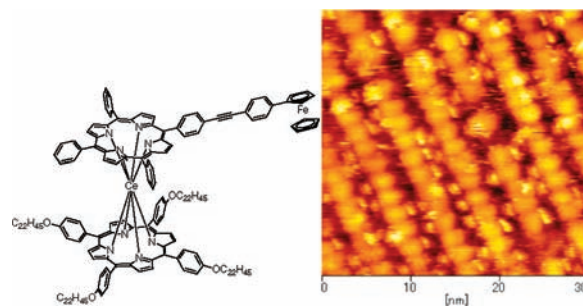


Figure 1. Ce double-decker porphyrin presenting a tethered ferrocene unit, [Ce(C₂₂OPP)(TPP-Fc)]. (Left) Molecular structure. (Right) STM image of a surface array at the HOPG-1-phenyloctane interface (20 μM; *I* = 10 pA; *V*_{sample} = −1.0 V).

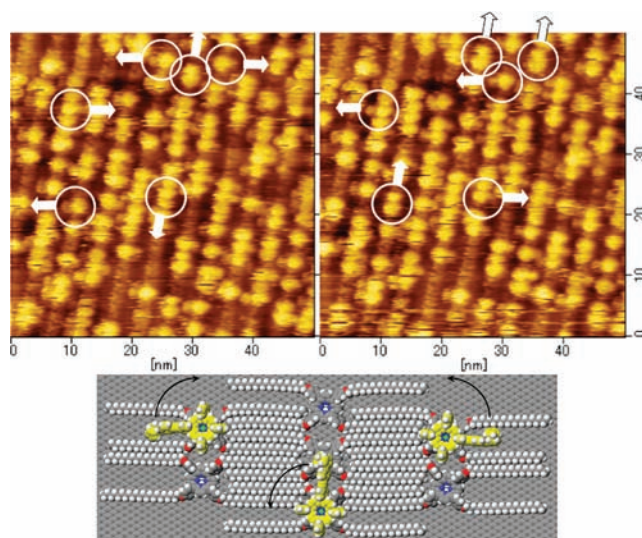


Figure 2. Mixed array of [Ce(C₂₂OPP)(TPP-Fc)] and H₂(C₂₂OPP) (10 μM/10 μM) at the HOPG-1-phenyloctane interface. (Top) STM images of the same area, one recorded immediately after the other (*I* = 10 pA; *V*_{sample} = −1.0 V). Encircled molecules changed their orientation during the interval; arrows indicate the orientation of the ferrocene units. (Bottom) Schematic representation of the three circled units in upper regions of the images.

due to double-decker porphyrins with a parallel ferrocene moiety (||). The right-hand image in Figure 2 was taken immediately after (starting 86 s later) recording that on the left image, on the same area. Comparison of these images reveals that six of the double-decker molecules had reoriented between the first and second scans; the reorientation of the three grouped in the upper regions of the images are illustrated schematically in the lower panel. Thus, we have visualized the orientational changes of double-decker complexes in real space on an individual-molecule basis.

[†] Nihon University.

[‡] National Institute of Advanced Industrial Science and Technology.

We collected data for over 300 double-decker molecules from 25 scans (60–90 s for each) on six different samples to analyze the orientations and reorientations quantitatively. The double-decker molecules may be categorized into three classes according to their neighboring molecules: ones that are flanked by two free-base porphyrins (class 1), ones that are flanked by one free-base porphyrin and one double-decker molecule (class 2), and ones flanked by two double-decker molecules (class 3). Whereas the four antiprismatic orientations are equivalent in solution, the lamellar formation on the surface makes the perpendicular and parallel orientations nonequivalent. Table 1 lists the fractions of molecules in their respective orientations (P_{\perp} and P_{\parallel}). The perpendicular orientation is preferred over the parallel orientation; this preference is more pronounced in class 2 than in class 1. The orientational preference indicates that interaction of the ferrocene unit with the interstitial alkyl groups is favored over interaction with the free-base porphyrin. The different values of P_{\perp} and P_{\parallel} for classes 1 and 2 indicate that the neighboring molecules play a role in determining the orientation. Quantitatively, the perpendicular orientation is more stable than the parallel orientation by 2.1 ± 0.9 and 3.8 ± 1.2 kJ mol⁻¹ for molecules in classes 1 and 2, respectively, on the assumption of the Boltzmann distribution.

Assuming that the 90° flips of the double-decker molecules would follow a Poissonian process, the number of events per molecule in a unit time would correspond to the first-order rate constant. Table 1 summarizes the rate constants obtained after comparing the orientations of individual molecules in consecutive images.⁸ We found that the rate constants for the 90° flips differed depending on the initial orientation; from perpendicular to parallel, $k_{\perp \rightarrow \parallel}$ was ca. $(1-3) \times 10^{-3}$ s⁻¹; vice versa, $k_{\parallel \rightarrow \perp}$ was ca. 1×10^{-2} s⁻¹. These values are consistent with the perpendicular-to-parallel being perturbed by adjacent molecules, with the reverse process being less influenced. These aspects are unique to the surface assembly; they are not observable in solution.

Most of the orientational changes occurred when the STM tip was positioned away from the molecules, even though it passed immediately above them many times (typically, 10 times) during imaging. Increasing the tunnel current from 10 to 20 pA did not result in any detectable change in the rate of rotational libration, suggesting that it was thermally induced. Precise assessment of the effects of the tip and the scanning parameters was difficult, however, because the ranges of bias voltages and tunnel currents that produced clear images were rather narrow, preventing us from investigating the effects of these parameters beyond what is reported here.

Table 1. Orientation and Rotational Libration of [Ce(C₂₂OPP)(TPP-Fc)]^{a-c}

class	P_{\perp}	P_{\parallel}	$E_{\perp} - E_{\parallel}$ kJ mol ⁻¹	$k_{\perp \rightarrow \parallel}$ 10 ⁻³ s ⁻¹	$k_{\parallel \rightarrow \perp}$ 10 ⁻³ s ⁻¹
1	0.70 ± 0.08	0.30 ± 0.08	-2.1 ± 0.9	2.9 ± 0.8	9.5 ± 3.0
2	0.90 ± 0.04	0.10 ± 0.04	-3.8 ± 1.2	0.95 ± 0.36	8.7 ± 4.0

^a Errors indicated are 95% confidence intervals. ^b 25 ± 2 °C. ^c $I = 10$ or 20 pA; $V_{\text{sample}} = -1.00$ to -1.25 V.

In conclusion, we have visualized the rotational libration of a double-decker porphyrin by using a ferrocene unit as a molecular beacon signaling its position. STM observation of individual molecules revealed neighbor-dependent energetics and kinetics for

the rotational libration process. We are currently investigating the effects of molecular structures and intermolecular interactions on the rotational behavior of related double-decker complexes at the individual-molecule level.

Acknowledgment. This study was supported by the Asahi Glass Foundation, Nihon University (Nanotechnology Excellence), and the Ministry of Education, Culture, Sports, Science, and Technology, Japan (High-Tech Research Center Projects for Private Universities and Grant-in-Aid for Scientific Research).

Supporting Information Available: Experimental procedures and characterization of the compounds. This material is available free of charge via the Internet at <http://pubs.acs.org>.

References

- (a) Balzani, V.; Credi, A.; Venturi, M. *Molecular Devices and Machines: A Journey Into the Nanoworld*; Wiley-VCH: Weinheim, 2004. (b) *Molecular Switches*; Feringa, B. L., Ed.; Wiley-VCH: Weinheim, 2003. (c) Kottas, G. S.; Clarke, L. I.; Horinek, D.; Michl, J. *Chem. Rev.* **2005**, *105*, 1281–1376. (d) van Delden, R. A.; ter Wiel, M. K. J.; Pollard, M. M.; Vicario, J.; Koumura, N.; Feringa, B. L. *Nature* **2005**, *437*, 1337–1340.
- (a) Takeuchi, M.; Imada, T.; Ikeda, M.; Shinkai, S. *Tetrahedron Lett.* **1998**, *39*, 7897–7900. (b) Sugasaki, A.; Ikeda, M.; Takeuchi, M.; Robertson, A.; Shinkai, S. *J. Chem. Soc., Perkin Trans. 1* **1999**, 3259–3264. (c) Ikeda, M.; Takeuchi, M.; Shinkai, S.; Tani, F.; Naruta, Y. *Bull. Chem. Soc. Jpn.* **2001**, *74*, 739–746. (d) Ikeda, M.; Takeuchi, M.; Shinkai, S.; Tani, F.; Naruta, Y.; Sakamoto, S.; Yamaguchi, K. *Chem.–Eur. J.* **2002**, *8*, 5542–5550.
- (a) Tashiro, K.; Konishi, K.; Aida, T. *J. Am. Chem. Soc.* **2000**, *122*, 7921–7926. (b) Tashiro, K.; Konishi, K.; Aida, T. *Angew. Chem., Int. Ed.* **1997**, *36*, 856–858. (c) Tashiro, K.; Fujiwara, T.; Konishi, K.; Aida, T. *Chem. Commun.* **1998**, 1121–1122.
- (a) Otsuki, J.; Kawaguchi, T.; Yamakawa, T.; Asakawa, M.; Miyake, K. *Langmuir* **2006**, *22*, 5708–5715. (b) Miyake, K.; Fukuta, M.; Asakawa, M.; Hori, Y.; Ikeda, T.; Shimizu, T. *J. Am. Chem. Soc.* **2009**, *131*, 17808–17813.
- (a) Ye, T.; Takami, T.; Wang, R.; Jiang, J.; Weiss, P. S. *J. Am. Chem. Soc.* **2006**, *128*, 10984–14985. (b) Takami, T.; Arnold, D. P.; Fuchs, A. V.; Will, G. D.; Goh, R.; Waclawik, E. R.; Bell, J. M.; Weiss, P. S.; Sugiura, K.; Liu, W.; Jiang, J. *J. Phys. Chem. B* **2006**, *110*, 1661–1664. (c) Gómez-Segura, J.; Díez-Pérez, I.; Ishikawa, N.; Nakano, M.; Veciana, J.; Ruiz-Molina, D. *Chem. Commun.* **2006**, 2866–2868. (d) Klymchenko, A. S.; Slevin, J.; Binnemans, K.; De Feyter, S. *Langmuir* **2006**, *22*, 723–728. (e) Yang, Z.-Y.; Gan, L.-H.; Lei, S.-B.; Wan, L.-J.; Wang, C.; Jiang, J.-Z. *J. Phys. Chem. B* **2005**, *109*, 19859–19856. (f) Binnemans, K.; Slevin, J.; De Feyter, S.; De Feyter, F. C.; Donnio, B.; Guillon, D. *Chem. Mater.* **2003**, *15*, 3930–3938.
- For reorientation of molecules or molecular fragments, see: (a) Gimzewski, J. K.; Joachim, C.; Schlittler, R. R.; Langlais, V.; Tang, H.; Johannsen, I. *Science* **1998**, *281*, 531–533. (b) Vaughan, O. P. H.; Williams, F. J.; Bamos, N.; Lambert, R. M. *Angew. Chem., Int. Ed.* **2006**, *45*, 3779–3781. (c) Weigelt, S.; Busse, C.; Petersen, L.; Rauls, E.; Hammer, B.; Gothelf, K. V.; Besenbacher, F.; Linderoth, T. R. *Nat. Mater.* **2006**, *5*, 112. (d) Wahl, M.; Stöhr, M.; Spillmann, H.; Jung, T. A.; Gade, L. H. *Chem. Commun.* **2007**, 1349–1351. (e) Wintjes, N.; Bonifazi, D.; Cheng, F.; Kiebele, A.; Stöhr, M.; Jung, T.; Spillmann, H.; Diederich, F. *Angew. Chem., Int. Ed.* **2007**, *46*, 4089–4092. (f) Baber, A. E.; Tierney, H. L.; Sykes, E. C. H. *ACS Nano* **2008**, *2*, 2385–2391. (g) Lei, S.-B.; Deng, K.; Yang, Y.-L.; Zeng, Q.-D.; Wang, C.; Jiang, J.-Z. *Nano Lett.* **2008**, *8*, 1836–1843.
- Not all of the double-decker molecules appear to present a ferrocene unit; such molecules remained unaccompanied by a ferrocene unit in subsequent scans. This phenomenon might be due to upside-down adsorption or to irreversible changes in the ferrocene moiety caused by ambient STM; for an example of the latter, see: Yokota, Y.; Fukui, K.; Enoki, T.; Hara, M. *J. Phys. Chem. C* **2007**, *111*, 7561–7564.
- Exchange of molecules on the surface with those in solution was negligible. Replacement of [Ce(C₂₂OPP)(TPP-Fc)] or H₂(C₂₂OPP) units would have resulted in exchange in roughly half the time; we observed it occurring with a frequency as low as 6×10^{-3} s⁻¹ per molecule. Some orientational changes, such as 90° rotation followed by a -90° rotation, would have been missed in our counting approach. Nevertheless, the small fraction of molecules that changed their orientation at all, and the even smaller number that underwent 180° flips, between consecutive imaging suggest that the likelihood of orientational changes back and forth was also low. Quantitative analysis revealed that the effect was indeed much smaller than the error ranges indicated.

JA907077E